Supramolecular Assembly Formation of Ferrioxamine B and Its Al(III), Ga(III), and In(III) Analogues with Dicyclohexano-18-Crown-6 in Chloroform

I. Spasojević, I. Batinić-Haberle, P. L. Choo, and A. L. Crumbliss*

Contribution from the Department of Chemistry, Duke University, Box 90346, Durham, North Carolina 27708-0346

Received February 7, 1994®

Abstract: We have shown that the crown ether dicyclohexano-18-crown-6 recognizes the terminal amine group of deferriferrioxamine B (H_4DFB^+) and its Al(III), Ga(III), Fe(III), and In(III) complexes ($MHDFB^+$) by host–guest complex formation. Host–guest formation constants for these supramolecular assemblies in chloroform at 25 °C were determined as follows: log $K_a(H_4DFB^+)$ = 4.56, log $K_a(AlHDFB^+)$ = 3.48, log $K_a(GaHDFB^+)$ = 3.59, log K_a-($FeHDFB^+$) = 3.67, log $K_a(InHDFB^+)$ = 3.92. Chloroform extraction equilibrium constants (K_{ex}) for the extraction of the $MHDFB^+$ complexes and H_4DFB^+ in the presence of picrate anion by crown ether were determined as well as distribution constants (K_d) between a chloroform and aqueous phase in the absence of crown ether: log $K_{ex}(H_4DFB^+)$ = 2.89, log $K_{ex}(AlHDFB^+)$ = 2.43, log $K_{ex}(GaHDFB^+)$ = 2.84, log $K_{ex}(FeHDFB^+)$ = 3.05, log $K_{ex}(InHDFB^+)$ = 3.46; log $K_d(H_4DFB^+)$ = −1.66, log $K_d(AlHDFB^+)$ = −1.05, log $K_d(GaHDFB^+)$ = −0.75, log $K_d(FeHDFB^+)$ = −0.62, log $K_d(InHDFB^+)$ = −0.46. In the series $InHDFB^+$, $FeHDFB^+$, $GaHDFB^+$, and $AlHDFB^+$ there is increasing hydration in the second coordination shell, as suggested by a linear relationship between log (K_a,K_{ex},K_d) and $1/r_i$ (r_i = M^{3+} radius) and $M(H_2O)_6^{3+}$ hydration enthalpy (ΔH_{hyd}), which consequently increases hydrophilicity (decreases K_d) and increases steric hindrance to crown ether host–guest complex formation (decreases K_a). Correspondingly, the chloroform extraction constants ($K_{ex} = K_d \cdot K_a$), which depend on chloroform/water distribution (K_d) and host–guest complex formation (K_a), decrease in the same sequence. We conclude that the protonated amine of the free ligand H_4DFB^+ and its metal complexes provides a recognition site through formation of a supramolecular assembly with a crown ether. Second coordination shell effects (hydrophilicity) provide a mechanism to discriminate between different M(III) complexes of deferriferrioxamine B. The low K_d value obtained for deferriferrioxamine B distribution between the hydrophilic and lipophilic phase is consistent with previous reports concerning the therapeutic use of this ligand to remove intracellular iron from patients with iron overload.

Introduction

The mechanism for siderophore mediated cellular iron acquisition, which involves iron release from the Fe(III) complex and subsequent incorporation into the cell, is not yet fully understood.[1] As cell surface recognition factors may play a significant role in siderophore mediated iron bioavailability, macrocyclic ligands such as crown ethers with hydrophobic exteriors and hydrophilic interiors have been introduced as models for cell surface receptors.[2,3] Crown ethers are excellent hosts for alkali and alkaline earth cations, often demonstrating a high degree of cation selectivity. Therefore they resemble the naturally occurring antibiotic macrocycles which have been shown to alter the permeability of biological membranes to certain cations.[4-6] It has also been established that crown ethers with an appropriate cavity size recognize protonated amine side chains of biological molecules by host–guest complex formation.[5]

Crown ether cation selectivity is governed by the ion-cavity-radius concept as well as by the charge density of the metal cation, the nature (nucleophilicity) of the anion present, and by conformational energy aspects of the crown ether.[4,7-10] When host–guest complexation occurs in liquid systems the polarity of the solvent also makes a significant contribution to the complexing ability of the crown ether.[7,8]

An objective of the experiments described in this report is to examine the hypothesis that molecular recognition will occur for the Fe(III)–hydroxamate siderophore complex ferrioxamine B ($FeHDFB^+$) (**1**), through host–guest complex formation with the terminal alkylammonium functional group. Because of its molecular flexibility and adequate cavity size that can distinguish between ammonium and other cations present in our system to maintain a constant ionic strength, dicyclohexano-18-crown-6 (DC-18-C-6) (**2**) has been selected as the most suitable[7,11,12] of the crown ether family for our investigation.

Host–guest complex formation, represented by the equilibrium shown in eq 1, is of interest as a working model for molecular

$$MHDFB^+ + \text{DC-18-C-6} \rightleftharpoons (MHDFB^+, \text{DC-18-C-6}) \quad (1)$$

recognition of a metal transport complex by the cell surface. A schematic representation of host–guest complexation for ferrioxamine B is illustrated in **3**. A supramolecular assembly such as shown in **3** also provides a mechanism for extracting a highly hydrophilic complex from an aqueous phase to a lipophilic phase, and therefore has application in such areas as trace and precious metal recovery.

* Address correspondence to this author.

® Abstract published in *Advance ACS Abstracts*, June 1, 1994.

(1) Crumbliss, A. L. In *Handbook of Microbial Iron Chelates*; Winkelmann, G., Ed.; CRC Press: Boca Raton, FL. 1991; pp 177–233.
(2) Fyles, T. M. *Biorg. Chem. Front.* **1990**, *1*, 71–113.
(3) Fendler, J. H. *Chem. Eng. News* **1984**, *62*, 25–39.
(4) Lamb, J. D.; Christensen, J. J.; Izatt, S. R.; Bedke, K.; Astin, M. S.; Izatt, R. M. *J. Am. Chem. Soc.* **1980**, *102*, 3399–3403.
(5) Lehn, J.-M. *Angew. Chem., Int. Ed. Engl.* **1988**, *27*, 89–112.
(6) Pederson, C. *J. Angew. Chem., Int. Engl. Ed.* **1988**, *27*, 1021–1027.
(7) Poonia, N. S. Multidentate Macromolecules: Principles of Complexation with Alkali and Alkaline Earth Cations. In *Progress in Macrocyclic Chemistry*; Izatt, R. M., Christensen, J. J., Eds.; Wiley Interscience: New York, 1979; Vol. 1, Chapter 4.
(8) Smid, J. *Angew. Chem., Int. Ed. Engl.* **1972**, *11*, 112–127.
(9) Izatt, R. M.; Bradshaw, J. S.; Nielsen, S. A.; Lamb, J. D.; Christensen, J. J. *Chem. Rev.* **1985**, *85*, 271–339.
(10) Inoue, Y.; Gokel, G. W. *Cation Binding by Macromolecules*; Marcel Dekker, Inc.: New York and Basel, 1990.
(11) Pederson, C. J.; Frensdorff, H. K. *Angew. Chem., Int. Ed. Engl.* **1972**, *11*, 16–25.
(12) Crumbliss, A. L. *Coord. Chem. Rev.* **1990**, *105*, 155–179.

0002-7863/94/1516-5714$04.50/0

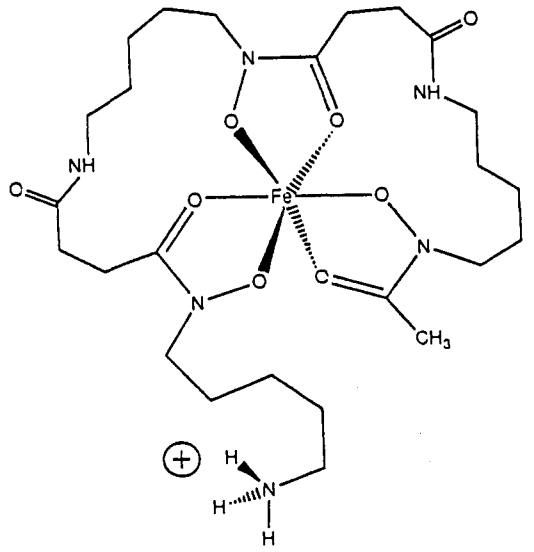

1

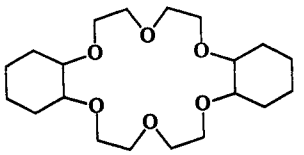

2

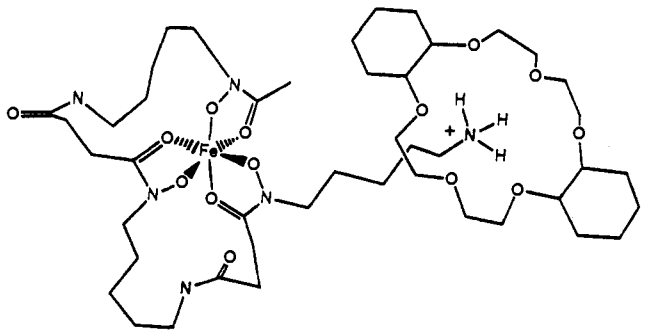

3

The approach taken to achieve our objective was to quantify and characterize the molecular recognition of ferrioxamine B and metal substituted ferrioxamine B complexes $MHDFB^+$ (M = Fe(III), Al(III), Ga(III), and In(III)) and a relevant related series of alkylammonium ions by dicyclohexano-18-crown-6 (CE). This has been accomplished by investigating the following water/chloroform extraction (eq 2), and corresponding distribution

$$RNH_3^+{}_{aq} + pic^-{}_{aq} + CE_{org} \rightleftharpoons (RNH_3^+,CE,pic^-)_{org} \qquad K_{ex}^{RNH_3^+,CE,pic^-} \quad (2)$$

$$K_{ex}^{RNH_3^+,CE,pic^-} = [(RNH_3^+,CE,pic^-)]_{org}/\{[RNH_3^+]_{aq}[pic^-]_{aq}[CE]_{org}\} \quad (3)$$

equilibrium in the absence of crown ether. RNH_3^+ represents $MHDFB^+$, H_4DFB^+, ammonium, and alkylammonium ions.

NH_4^+, $CH_3(CH_2)_4NH_3^+$ (pentylamine), and deferriferrioxamine B (H_4DFB^+) extraction experiments were conducted to determine the influence of both alkyl and hydroxamate substituent groups on host–guest complex formation between RNH_3^+ and dicyclohexano-18-crown-6. We wished to further consider whether the metal center, with its static first and dynamic second coordination sphere, might play a role in metal complex–crown ether supramolecular assembly formation. Therefore, experiments were undertaken with aluminum(III)–, gallium(III)–, and indium(III)–deferriferrioxamine B complexes as well as iron(III). All of these metals are of biological importance[13] and show similarities in their aqueous coordination chemistry.[14-17] Members of this series of spherically symmetrical 3+ metal ions (no crystal field stabilization energy as a result of d^0, d^{10}, and high-spin d^5 electron configurations) all form stable complexes of similar structure with monohydroxamic[18,19] and trihydroxamic acids.[20] Stability constants for their complexes[14,16] as well as their kinetic parameters[15,21-24] differ significantly as a result of their different size[25] and electronegativity.[26] Picrate anion (pic^-) was selected as the counter ion in our studies due to the fact that it is weakly nucleophilic and highly lipophilic and therefore forms strong ion pairs with cations in nonaqueous solvents.[4,7] Mg^{2+} cation was used to maintain constant ionic strength, due to its low extractibility into the chloroform phase by dicyclohexano-18-crown-6 and therefore negligible tendency to compete with $MHDFB^+$ extraction.[7,10,27]

Experimental Section

Materials. Aqueous Solutions. Picric acid, obtained from Aldrich, was recrystallized from water.[28] *Extreme care should be taken while working with both picric acid and picrate salts.* Crystalline sodium picrate was prepared from picric acid and sodium hydroxide and recrystallized twice from absolute ethanol and ethanol/water mixture.[29] Magnesium picrate stock solution was prepared by neutralizing either $MgCO_3$, $Mg(OH)_2{\cdot}5H_2O$ (Sigma), or $Mg(OH)_2$ (Aldrich) with a saturated aqueous solution of picric acid.[30,31] The purity of the crystals of picric acid and sodium picrate and the concentration of the aqueous stock solution of magnesium picrate were determined spectrophotometrically, using $\epsilon_{picrate} = 1.44 \times 10^4\ cm^{-1}\ M^{-1}$ at 356 nm.[32] The molar absorptivity of magnesium picrate in aqueous solution was checked by determining the magnesium picrate concentration by two methods. In the first method, an aliquot of the solution was passed through an anion exchange resin (AG 1-X8, Bio-Rad; nitrate form) to eliminate the picrate and then through Dowex 50 W-X8 cation exchange resin (J. T. Baker). The concentration of the released HNO_3 was determined by titration with NaOH. In the second method, an aliquot of the magnesium picrate solution was passed through a cation exchange resin, and the liberated picric acid titrated with NaOH. The results obtained by the two methods are in excellent agreement with spectrophotometric data for aqueous picrate ion.

Magnesium nitrate stock solution was prepared by neutralizing $MgCO_3$ and $Mg(OH)_2{\cdot}5H_2O$ with 70% nitric acid (Mallinckrodt).[33] $Mg(NO_3)_2$,

(13) daSilva, J. J. R.; Williams, R. J. P. *The Biological Chemistry of Elements*; Clarendon Press: Oxford, 1991.
(14) Evers, A.; Hancock, R. D.; Martell, A. E.; Motekaitis, R. J. *Inorg. Chem.* **1989**, *28*, 2189–2195.
(15) Crumbliss, A. L.; Garrison, J. M. *Comments Inorg. Chem.* **1988**, *8*, 1–26.
(16) Borgias, B.; Hugi, A. D.; Raymond, K. N. *Inorg. Chem.* **1989**, *28*, 3538–3545.
(17) Burgess, J. *Metal Ions in Solution*, Ellis Horwood Series in Chemical Science; Chichester, Sussex, 1978.
(18) Dietrich, A.; Fidelis, K. A.; Powell, D. R.; Van der Helm, D.; Eng-Wilmot, D. L. *J. Chem. Soc., Dalton Trans.* **1991**, 231–239.
(19) Borgias, B. A.; Barclay, S. J.; Raymond, K. N. *J. Coord. Chem.* **1986**, *15*, 109–123.
(20) Van der Helm, D.; Baker, J. R.; Loghry, R. A.; Ekstrand, J. D. *Acta Crystallogr.* **1981**, *B37*, 323–330.
(21) Monzyk, B.; Crumbliss, A. L. *J. Am. Chem. Soc.* **1982**, *104*, 4921–4929.
(22) Biruš, M.; Bradić, Z.; Krznarić, G.; Kujundžić, N.; Pribanić, M.; Wilkins, P. C.; Wilkins, R. G. *Inorg. Chem.* **1987**, *26*, 1000–1005.
(23) Garrison, J. M.; Crumbliss, A. L. *Inorg. Chim. Acta* **1987**, *138*, 61–65.
(24) Batinić-Haberle, I.; Biruš, M.; Imper-Vuletić, V.; Spasojević, I. *Croat. Chem. Acta* **1993**, *66*, 373–383.
(25) Allred, A. L. *J. Inorg. Nucl. Chem.* **1961**, *17*, 215–221.
(26) Shannon, R. D. *Acta Crystallogr.* **1976**, *A32*, 751.
(27) Izatt, R. M.; Nelson, D. P.; Rytting, J. H.; Haymore, B. L.; Christensen, J. J. *J. Am. Chem. Soc.* **1976**, *98*, 7620–7626.
(28) Ouchi, M.; Inoue, Y.; Kanzaki, T.; Hakushi, T. *J. Org. Chem.* **1984**, *49*, 1408–1412.
(29) Coplan, A. M.; Fuoss, R. M. *J. Phys. Chem.* **1964**, *68*, 1177–1180.
(30) Nakagawa, K.; Amita, K.; Mizuno, H.; Inoue, Y.; Hakushi, T. *Bull. Chem. Soc. Jpn.* **1987**, *60*, 2037–2040.
(31) Wong, K. H.; Ng, H. L. *J. Coord. Chem.* **1981**, *11*, 49–55.
(32) Sadakane, A.; Iwachido, T.; Toei, K. *Bull. Chem. Soc. Jpn.* **1975**, *48*, 60–63.

$NaNO_3$ (Sigma), and NH_4NO_3 (Fisher) concentrations were determined by passing an aqueous solution through a cation exchange resin and titrating the acid liberated with NaOH.

An ammonium picrate solution was prepared by mixing ammonium nitrate and magnesium picrate stock solutions. A pentylamine picrate solution was prepared by neutralizing pentylamine (Aldrich) with picric acid up to pH ~5.6. The picrate concentration, equal to the pentylamine concentration, was determined spectroscopically using the molar absorptivity of aqueous picrate. A deferriferrioxamine B/magnesium picrate solution was prepared by dissolving the mesylate salt (Sigma) in water with subsequent addition of $Mg(pic)_2$ stock solution.

Deferriferrioxamine B complexes of iron(III), aluminum(III), gallium(III), and indium(III) were all prepared by the same method. For example, an iron(III) stock solution[34] was mixed with deferriferrioxamine B at pH ~ 1. After equilibration the pH was raised to 6 with the addition of solid $Mg(OH)_2$. Eventually, a stock solution of either $Mg(NO_3)_2$ or $Mg(pic)_2$ was added to adjust the ionic strength and to provide the appropriate counter anion for the extraction experiments. The concentration of $FeHDFB^+$ was determined by UV–vis spectroscopy ($\epsilon = 2.6 \times 10^3$ cm^{-1} M^{-1} at 425 nm).[21] The concentrations of $AlHDFB^+$, $InHDFB^+$, and $GaHDFB^+$ were determined by noting that Al(III),[22] In(III), and Ga(III)[35,36] can be successfully exchanged with Fe(III) to form $FeHDFB^+$, which was monitored spectrophotometrically.

Twice distilled water was used in all experiments. Throughout the extraction procedures, water saturated with chloroform (Spectroscopic Grade, Fisher Scientific) and chloroform saturated with water were used.

Chloroform Solutions. *cis*-DC-18-C-6, a mixture of *cis*, *syn*, *cis* and *cis*, *anti*, *cis* isomers, was used as obtained from Aldrich. Chloroform solutions were made by dissolving appropriate amounts of DC-18-C-6 in a known volume of $CHCl_3$.

Methods. The extraction procedure was accomplished by vigorously shaking, in a screw-cap glass vial equipped with a stir bar, equal volumes of the following: (1) an aqueous layer containing fixed amounts of M^{n+} or RNH_3^+ and the appropriate background electrolyte (picrate or nitrate salt, $I = 0.1$) and (2) a chloroform layer containing variable amounts of crown ether (usually 0.1–500 mM). After the layers were equilibrated for 14 h, they were centrifuged and separated. Both layers were treated as described below under Extraction Equilibria. The distribution of RNH_3^+ between the aqueous and chloroform phases was also determined in the absence of crown ether by the same method. Both the extraction and distribution of $AlHDFB^+$ were performed at pH 5.6 and 7.9 with no detectable difference in the results. Therefore, all experimental results reported here were determined at pH ~ 5.6.

Spectrophotometric measurements were made using Beckman Acta III and Varian Cary 2300 UV–vis spectrophotometers. All results reported are based on 3–5 independent determinations at 25.0 ± 0.5 °C. The ionic strength was kept at 0.1 M in all experiments by addition of $Mg(NO_3)_2$, $Mg(pic)_2$, $NaNO_3$, or Na(pic).

Molar absorptivities of the crown ether complexes with picrate salts in $CHCl_3$ were obtained from separate extraction runs in which the picrate concentration in the organic phase was taken to be equal to the difference between the total concentration and that found in the aqueous solution. Molar absorptivity values are as follows (average error 2.2%): DC-18-C-6·magnesium picrate ($\epsilon = 3.98 \times 10^4$ cm^{-1} M^{-1} at 370 nm); DC-18-C-6·sodium picrate ($\epsilon = 1.69 \times 10^4$ cm^{-1} M^{-1} at 367 nm); DC-18-C-6·ammonium picrate ($\epsilon = 1.61 \times 10^4$ cm^{-1} M^{-1} at 364 nm); DC-18-C-6·pentylamine picrate ($\epsilon = 1.99 \times 10^4$ cm^{-1} M^{-1} at 375 nm); and DC-18-C-6·deferriferrioxamine B picrate ($\epsilon = 2.29 \times 10^4$ cm^{-1} M^{-1} at 370 nm). The molar absorptivity for the (DC-18-C-6·$H_4DFB^+pic^-$) in chloroform was determined differently, since in that case aqueous picrate concentration did not equal the cation concentration. After the equilibrium was achieved, an aliquot of the aqueous layer was passed through an anion exchange resin to eliminate picrate and rinsed from the column until reaction with Fe^{3+} to detect the presence of H_4DFB^+ was negative. The solution was collected in a volumetric flask, followed by the addition of Fe(III) stock solution, and the pH was kept at ~3.6. The concentration of $FeHDFB^+$ was determined by UV–vis spectroscopy, as described above. The picrate concentration in the organic phase equals the organic phase H_4DFB^+ concentration, and therefore the molar absorptivity of DC-18-C-6·$H_4DFB^+pic^-$ may be calculated from the expression $\epsilon = A/([H_4DFB^+]_0 - [H_4DFB^+]_{aq})$ (0 = initial, path length = 1.0 cm).

Ferrioxamine B extraction was accomplished, both with nitrate and with picrate as the counterion. Extraction of NH_4^+, pentylamine, deferriferrioxamine B, $AlHDFB^+$, $GaHDFB^+$, and $InHDFB^+$ were all done with picrate as the counter anion. At low picrate concentrations, $Mg(NO_3)_2$ was used to maintain a constant ionic strength of 0.1 M. The extraction of (Mg^{2+}, NO_3^-) from the aqueous to the chloroform layer can be neglected in relation to the cation of primary interest.[4,10] The initial concentrations of cations used throughout the experiments were 8.9×10^{-3} M (Na^+), 3.33×10^{-2} M (Mg^{2+}), and 7.1×10^{-4}–6×10^{-3} M (RNH_3^+). Nitrate concentration was 8.9×10^{-3}–6.66×10^{-2} M, and picrate was 7.1×10^{-4}–6.66×10^{-2} M. Crown ether concentrations ranged from 10^{-4} M to 5×10^{-1} M depending upon the extractibilities of the cations present.

A short hand notation is used below in the description of the extraction equilibrium and distribution equilibrium experiments which allows for easy reference. **Cation^{n+}/*cation*$^{n+}$//anion/*anion*** relates to the extraction of the cation of primary interest (listed first) from the aqueous to the chlorofom phase; the second cation listed is present for the purpose of maintaining a constant ionic strength. Both cations are present with their corresponding anions listed first and second, respectively. The Roman numerals designate a particular extraction or distribution equilibrium system, which is then referred to in the Results and Discussion sections.

Extraction Equilibria. The extraction of Mg^{2+} was expected to be very low and any impurities which have extraction equilibrium constants several orders of magnitude higher can introduce significant errors. Therefore, alkali metals were eliminated from the Mg^{2+} picrate stock solution by prior extraction with 0.1 M DC-18-C-6 in $CHCl_3$. The aqueous and organic layers were shaken vigorously, left to equilibrate overnight, and separated. The picrate concentration in the aqueous layer was checked, and this layer was used for all of the extraction equilibrium constant determinations.

Mg^{2+}//Picrate (I) and Na^+/*Mg^{2+}*//Picrate/*Nitrate* (II). Independent extraction extraction experiments for Mg^{2+} in the absence of RNH_3^+ are used to correct the overall extraction experimental data for Mg^{2+} complexation by crown ether and to confirm the expected 1:1 Mg^{2+}/crown ether stoichiometry. Equilibrium concentrations of sodium and magnesium in both layers were calculated by measuring the picrate concentration.

NH_4^+/*Mg^{2+}*//Picrate/*Nitrate*(III), $CH_3(CH_2)_4NH_3$/*Mg^{2+}*//Picrate/Nitrate (IV), and H_4DFB^+/*Mg^{2+}*//Picrate (V). The equilibrium concentrations of NH_4^+, pentylamine, and H_4DFB^+ were calculated by measuring picrate concentrations in the organic layer. In the case of H_4DFB^+ extraction, in addition to calculating the aqueous concentration as the difference between the initial and organic equilibrium concentrations, the H_4DFB^+ concentration in the aqueous layer was also measured. Both methods provided equivalent results.

$FeHDFB^+$/*Mg^{2+}*//Picrate (VI) and $FeHDFB^+$/*Mg^{2+}*//Nitrate (VII). $FeHDFB^+$ concentration was determined in both layers, and in the case of (VI) the picrate concentration was determined as well. Picrate has a large molar absorptivity, which prevents ferrioxamine B determination in its presence. Thus, the picrate concentration was first determined in both layers after appropriate dilution. Afterwards, a part of the aqueous layer was passed through an anion exchange resin (nitrate form) to eliminate picrate and diluted to the appropriate volume, and the $FeHDFB^+$ concentration was determined spectrophotometrically. In order to determine the ferrioxamine B concentration in the chloroform layer, a reverse extraction was done. Namely, a part of the chloroform layer was vigorously shaken with 0.1 M KNO_3. K^+ has a significantly higher affinity than NH_4^+ for the DC-18-C-6 cavity[37] and can completely replace $FeHDFB^+$ in the crown ether assembly, thereby displacing $FeHDFB^+$ into the aqueous phase. An aliquot of the aqueous phase was treated with anion exchange resin in the nitrate form, and $FeHDFB^+$ was determined spectrophotometrically as described above. Nitrate did not interfere with the ferrioxamine B determination.

$MHDFB^+$/*Mg^{2+}*//Picrate (VIII). After equilibrium was established, the picrate and $MHDFB^+$ concentrations were determined in both layers by a procedure similar to that described above for $FeHDFB^+$ extraction. The metal complex concentration in the organic layer was determined by an interchange reaction with Fe(III), after the organic layer was treated with KNO_3, and all the complex was transferred into an aqueous phase. An aliquot of the aqueous phase was passed through an anion exchange resin, and Fe(III) stock solution was added in excess. The metal exchange was allowed to go to completion, and the $FeHDFB^+$ concentration was measured spectrophotometrically as described above.

Distribution Equilibria. Distribution equilibria were measured by a method similar to that described elsewhere[38] for the distribution of NH_4^+ and *t*-$BuNH_3^+$ picrates between aqueous and $CDCl_3$ layers.

$CH_3(CH_2)_4NH_3^+$/*Mg^{2+}*//Picrate/*Nitrate* (IV). A 10-mL aqueous solution of the same composition as used in the extraction procedure was vigorously shaken with 10 mL of $CHCl_3$. The layers were allowed to

(33) Mellor, J. W. *A Comprehensive Treatise on Inorganic Chemistry*; Longmans, Green and Co.: London, 1923; Vol. 4, p 379.

equilibrate for 14 h, and the $CHCl_3$ layer was transferred carefully to another separatory funnel. The organic picrate was reextracted to the aqueous phase with an equal volume of 0.1 M KNO_3, and its concentration in the aqueous phase, which equals the pentylamine concentration, was determined using $\epsilon = 1.44 \times 10^4$ cm^{-1} M^{-1} at $\lambda_{max} = 356$ nm.[32]

H_4DFB^+/Mg^{2+}//Picrate (V). Chloroform (10 mL) was shaken vigorously with 10 mL of an aqueous solution containing 2×10^{-2} M H_4DFB^+, 6.66×10^{-2} M picrate, and 3.33×10^{-2} M Mg^{2+}. The layers were allowed to separate and clarify for 14 h. The concentration of picrate in the chloroform phase, which equals the concentration of H_4DFB^+, was determined in the same way as described above for the pentylamine picrate determination.

MHDFB$^+$/Mg^{2+}//Picrate (VIII). Aliquots of aqueous solutions of $MHDFB^+$ were shaken vigorously with equal volumes of $CHCl_3$. After the organic and aqueous layers were equilibrated, they were separated, and an aliquot of the organic layer was shaken with a 5-fold volume excess of 0.1 M KNO_3. The remainder of the procedure for colorless complexes of Al, Ga, and In was the same as described for the pentylamine picrate distribution equilibrium determination (IV). The procedure for $FeHDFB^+$, after its reextraction into the aqueous phase, was the same as described under extraction equilibria for $FeHDFB^+/Mg^{2+}$//picrate (VI).

DC-18-C-6. The distribution equilibrium for DC-18-C-6 was determined according to the procedure of Frensdorff.[39] The value obtained for the equilibrium between $CHCl_3$ and water, $(DC\text{-}18\text{-}C\text{-}6)_{org} \rightleftharpoons (DC\text{-}18\text{-}C\text{-}6)_{aq}$, $K_d' = (6.3 \pm 0.7) \times 10^{-4}$, is in excellent agreement with the value published for the more polar solvent CH_2Cl_2, $K_d' = 2.6 \times 10^{-4}$,[39] where the ether is expected to be slightly more soluble.

Results

Overall Extraction Equilibria. The overall extraction equilibrium investigated may be written as follows:

$$RNH_3^+{}_{aq} + M^{n+}{}_{aq} + (n+1)pic^-{}_{aq} + 2CE_{org} \overset{K_{overall}}{\rightleftharpoons} (RNH_3^+,CE,pic^-)_{org} + (M^{n+},CE,npic^-)_{org} \quad (4)$$

where $RNH_3^+ = NH_4^+$ (III), $CH_3(CH_2)_4NH_3^+$ (IV), H_4DFB^+ (V), and $MHDFB^+$ (VI–VIII), CE = DC-18-C-6, and $M^{n+} = Mg^{2+}$ or Na^+. The function of the magnesium or sodium picrate is to permit all experiments to be carried out at a constant ionic strength ($I = 0.1$). The overall extraction experiment may be conceptually broken down into two extraction equilibria involving RNH_3^+ (eqs 2 and 3) and M^{n+} (eqs 5 and 6).

$$M^{n+}{}_{aq} + npic^-{}_{aq} + CE_{org} \rightleftharpoons (M^{n+},CE,npic^-)_{org} \qquad K_{ex}^{M^{n+},CE,npic^-} \quad (5)$$

$$K_{ex}^{M^{n+},CE,npic^-} = [(M^{n+},CE,npic^-)_{org}]/\{[M^{n+}]_{aq}[pic^-]_{aq}{}^n[CE]_{org}\} \quad (6)$$

The overall extraction constant ($K_{overall}$) may then be expressed as the product of the extraction constants for the individual equilibria of interest as shown in eq 7.

$$K_{overall} = (K_{ex}^{RNH_3^+,CE,pic^-}) \cdot (K_{ex}^{M^{n+},CE,npic^-}) \quad (7)$$

Independent extraction experiments for Mg^{2+} in the absence of RNH_3^+ (eq 5) are used to correct the overall extraction experimental data ($K_{overall}$) for CE complexation by Mg^{2+}. Equation 7 can then be used to compute $K_{ex}^{RNH_3^+,CE,pic^-}$ for reaction 2. Results obtained using this experimental approach are described in the following paragraphs.

Mg^{2+}//Picrate (I) and Na^+/Mg^{2+}//Picrate/Nitrate (II). There are few data available in the literature for the extraction of Mg^{2+} from an aqueous to an organic phase using macrocycles.[7,10,27,40-47] The high hydration energy keeps cations of small ionic radius and high charge such as Mg^{2+} partly hydrated, even in hydrophobic solvents.[45] No significant extraction of Mg^{2+} with Cl^-, ClO_4^-, or NO_3^- anions has been found, but with the "soft" picrate anion 2.5% Mg^{2+} extraction with 18-crown-6 into CH_2Cl_2 has been reported.[41] In contrast, the log extraction constant for the extraction of sodium picrate to $CDCl_3$ by dicyclohexano-18-crown-6 was reported to be 3.61.[48] Therefore, Mg^{2+} salts are not expected to effectively compete with the metal complexes ($MHDFB^+$) investigated in this study of crown ether extraction into a chloroform phase.

The extraction of magnesium salts into chloroform by DC-18-C-6 was quantified in our study in order to (1) correct the overall extraction experimental data for crown ether complexation of electrolyte cations; (2) confirm the expected 1:1 Mg^{2+}/CE stoichiometry; and (3) confirm the advantage of using Mg^{2+} rather than Na^+ salts for ionic strength control at our experimental conditions. Therefore, the extraction constants for both Mg(pic)$_2$ ($K_{ex}^{Mg^{2+},CE,2pic^-}$) and Na(pic) ($K_{ex}^{Na^+,CE,pic^-}$) were determined as illustrated in eqs 5 and 6, where M^{n+} is either Na^+ or Mg^{2+}. If Mg^{2+} is accompanied with nitrate as the counterion (II), its extraction may be neglected.[4] When the organic phase is apolar such as chloroform, there will be essentially no dissociation of the ion pairs in the organic phase. Since the DC-18-C-6 distribution constant between $CHCl_3$ and water ensures that >99.9% of the crown ether is in the organic phase (K_d' for $(DC\text{-}18\text{-}C\text{-}6)_{org} \rightleftharpoons (DC\text{-}18\text{-}C\text{-}6)_{aq}$ is $(6.3 \pm 0.7) \times 10^{-4}$), its concentration in the aqueous layer as well as host–guest complexation in the aqueous phase may be neglected. A 1:1 stoichiometry has been demonstrated for binding NH_4^+ with different crown ethers[10] and for the extraction of protonated primary and secondary amines with 18-C-6 into 1,2-dichloroethane.[49] The same stoichiometry was initially assumed in our experiments for $MHDFB^+$, and also for Mg^{2+},[7] and was later confirmed by our results.

A rearranged form of the extraction equilibrium constant ($K_{ex}^{M^{n+},CE,npic^-}$) in eq 6 may be written as follows

$$K_{ex}^{M^{n+},CE,npic^-} = D_M{}^{n+}/\{[pic^-]_{aq}[CE]_{org}\} \quad (8)$$

where

$$D_M{}^{n+} = [M^{n+},CE,npic^-]_{org}/[M^{n+}]_{aq} \quad (9)$$

$$[pic^-]_{aq} = [pic^-]_0 - [pic^-]_{org} \quad (10)$$

$$[CE]_{org} = [CE]_0 - [pic^-]_{org} \quad (11)$$

and $[pic^-]_0$ and $[CE]_0$ denote initial concentrations of picrate and

(34) Monzyk, B.; Crumbliss, A. L. *J. Am. Chem. Soc.* **1979**, *101*, 6203–6213.
(35) Spasojević, I., unpublished results.
(36) Emery, T. *Biochemistry* **1986**, *25*, 4629–4633.
(37) Frensdorff, H. K. *J. Am. Chem. Soc.* **1971**, *93*, 600–606.
(38) Moore, S. S.; Tarnowski, T. L.; Newcomb, M.; Cram, D. L. *J. Am. Chem. Soc.* **1977**, *99*, 6398–6405.
(39) Frensdorff, H. K. *J. Am. Chem. Soc.* **1971**, *93*, 4684–4688.
(40) Bogat-skii, A. V.; Luk'yanenko, N. G.; Mamina, M. U.; Shapkin, V. A.; Taubert, D. *Dokl. Akad. Nauk SSSR* **1989**, *250*, 1389–1392.
(41) Inoue, Y.; Ouchi, M.; Hakushi, T. *Bull. Chem. Soc. Jpn.* **1985**, *58*, 525–530.
(42) Chen, L.; Bos, M.; Grootenhuis, P. D. J.; Christenhusz, A.; Hoogendam, E.; Reinhoudt, D. N.; Van der Linden, W. E. *Anal. Chim. Acta* **1987**, *201*, 117–125.
(43) Izatt, R. M.; Clark, G. A.; Lamb, J. D.; King, J. E.; Christensen, J. J. *Thermochim. Acta* **1986**, *97*, 115–126.
(44) Izatt, R. M.; Pawlak, K.; Bradshaw, J. S.; Bruening, R. L. *Chem. Rev.* **1991**, *91*, 1721–2085.
(45) Iwachido, T.; Minami, M.; Sadakane, A.; Toei, K. *Chem. Lett.* **1977**, 1511–1514.
(46) Massaux, J.; Roland, G.; Desreux, J. F. *Inorg. Chim. Acta* **1982**, *60*, 129–133.
(47) Takeda, Y.; Matsumoto, Y.; *Bull. Chem. Soc. Jpn.* **1987**, *60*, 2313–2317.
(48) Koenig, K. E.; Lein, G. M.; Stuckler, P.; Kaneda, T.; Cram, D. J. *J. Am. Chem. Soc.* **1979**, *101*, 3553–3566.
(49) Noguchi, H.; Yoshio, M.; Kawahara, K.; Nakamura, H.; Magamatsu, M. *Anal. Lett.* **1980**, *13*, 217–281.

Table 1. Extraction (K_{ex}), Distribution (K_d), and Host–Guest Association Equilibrium Constants (K_a) As Defined in Eqs 12, 15, and 17[a]

cation		K_{ex}, M^{-2}	K_d, M^{-1}	K_a, M^{-1}
Mg^{2+}		12.36[b]		
Na^+		1.71×10^3	1.74×10^{-3} [c]	9.83×10^5
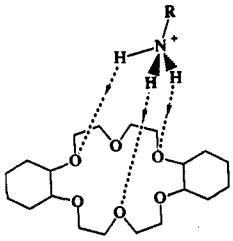 R =	H–	1.98×10^5	4.02×10^{-3} [c]	4.90×10^7
	CH_3–	1.20×10^5 [c]	1.45×10^{-2} [c]	8.31×10^6 [c]
	$(CH_3)_3C$–	3.13×10^4 [c]	2.37×10^{-1} [c]	1.32×10^5 [c]
	$CH_3CH_2CH_2CH_2CH_2$–	7.57×10^6	5.29×10^0	1.43×10^6
	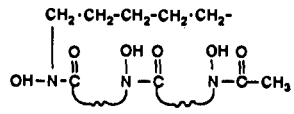	7.83×10^2	2.17×10^{-2}	3.61×10^4
	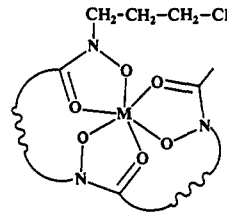 M = In(III)	2.85×10^3	3.5×10^{-1}	8.31×10^3
	Fe(III)	1.12×10^3	2.4×10^{-1}	4.68×10^3
	Ga(III)	6.88×10^2	1.8×10^{-1}	3.89×10^3
	Al(III)	2.71×10^2	9.0×10^{-2}	3.02×10^3

[a] Data collected at 25 ± 0.5 °C, I = 0.1 M ($Mg(pic)_2$ and $Mg(NO_3)_2$), accompanying anion = picrate; values given are an average of 3–5 independent determinations with an average error for K_{ex} of 1.5% except for $GaHDFB^+$ (0.6%) and $InHDFB^+$ (2%) and for K_d of 11%. [b] K, M^{-3}. [c] Data from ref 48.

crown ether, respectively. Plots of $D_{M^{n+}}$ *vs* $\{[pic^-]_{aq}[CE]_{org}\}$ are linear with slopes that correspond to $K_{ex}^{M^{n+},CE,pic^-}$. The intercepts are zero within experimental error, except when the magnesium picrate was not purified as described in the Experimental Section and a positive intercept was observed. This suggests the possibility of using crown ethers for the selective purification of different alkaline earth metal solutions. The linear plots confirm the 1:1 M^{n+}/DC-18-C-6 stoichiometry.

Values for $K_{ex}^{M^{n+},CE,npic^-}$ are given in Table 1. These results illustrate the advantage of using magnesium picrate rather than sodium picrate as supporting electrolyte, since apparently Mg^{2+} cannot significantly interfere with the extraction of ammonium and substituted ammonium cations by DC-18-C-6.

NH_4^+/*Mg^{2+}*//Picrate/*Nitrate* (III), $CH_3(CH_2)_4NH_3^+$/*Mg^{2+}*//Picrate/*Nitrate* (IV), and H_4DFB^+/*Mg^{2+}*//Picrate (V). A rearranged form of the extraction equilibrium constant ($K_{ex}^{RNH_3^+,CE,pic^-}$; eq 3) for equilibrium 2 may be written as follows

$$K_{ex}^{RNH_3^+,CE,pic^-} = D_{RNH_3^+}/\{[pic^-]_{aq}[CE]_{org}\} \quad (12)$$

where

$$D_{RNH_3^+} = [RNH_3^+,CE,pic^-]_{org}/[RNH_3^+]_{aq} = \{K_{overall}/K_{ex}^{Mg^{2+},CE,2pic^-}\}[pic^-]_{aq}[CE]_{org} = \{K_{ex}^{RNH_3^+,CE,pic^-}\}[pic^-]_{aq}[CE]_{org} \quad (13)$$

Equations 8–11 were used to calculate the cation distribution between the organic and aqueous phases, free crown ether concentration in the organic phase, and picrate concentration in the aqueous phase. Plots of $D_{RNH_3^+}$ *vs* $\{[pic^-]_{aq}[CE]_{org}\}$ gave a straight line. From eq 13 it is evident that the slope of this plot represents the extraction equilibrium constant ($K_{ex}^{RNH_3^+,CE,pic^-}$) for the species whose distribution is presented on the Y axis. The linearity of the plot confirms the stoichiometry shown in eq 2. Extraction constants for RNH_3^+ ($K_{ex}^{RNH_3^+,CE,pic^-}$) obtained in this way are compiled in Table 1.

$FeHDFB^+$/*Mg^{2+}*//Picrate (VI) and $FeHDFB^+$/*Mg*//Nitrate (VII). The overall extraction equilibrium for VI is expressed as shown in eq 4 with RNH_3^+ = $FeHDFB^+$. A plot of D_{FeHDFB^+} *vs*

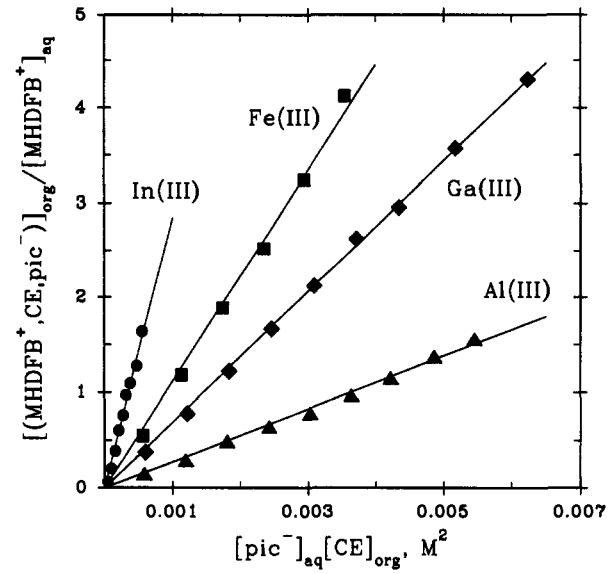

Figure 1. Plots of $[MHDFB^+,CE,pic^-]_{org}/[MHDFB^+]_{aq}$ (=D_{MHDFB^+}) as a function of $\{[pic]_{aq}[CE]_{org}\}$ according to eq 12 for $MHDFB^+$ extraction with picrate by DC-18-C-6 (CE) into $CHCl_3$, I = 0.1 M ($Mg(pic)_2$), T = 25 ± 0.5 °C, M = Al(III) (triangles), Ga(III) (rombs), Fe(III), (squares), and In(III) (circles).

$\{[pic^-]_{aq}[CE]_{org}\}$ according to eq 12 gives a straight line as illustrated in Figure 1. This confirms the 1:1 stoichiometry described in eq 2. The results for $K_{ex}^{FeHDFB^+,CE,pic^-}$ obtained from the slope of this plot are given in Table 1. From the results given in Table 1 it is evident that magnesium picrate extraction represents only 1% of the observed $FeHDFB^+(pic^-)$ extraction by DC-18-C-6. It is expected that magnesium extraction accompanied by nitrate counterion would be far less efficient, for the reasons already discussed. Neglecting magnesium nitrate extraction, the extraction constant for ferrioxamine B in the presence of nitrate anion ($K_{ex}^{FeHDFB^+,CE,NO_3^-}$) is 4.0 (±0.2) × 10^{-2} M^{-2}. This is considerably smaller than the extraction constant observed in the presence of picrate anion, consistent with the difference in lipophilicities of these two anions. The contribution of the nature of the anion ("soft" or "hard") to the extraction

efficiency of $FeHDFB^+$ is seen in the almost five orders of magnitude increase of the extraction equilibrium constant when nitrate is displaced with picrate (Table 1). At 0.05 M DC-18-C-6 concentration, 79% of $FeHDFB^+$ was extracted into the chloroform layer with picrate present and *ca.* 0.01% when nitrate was the counter ion.

Comparison of the K_{ex} for sodium picrate extraction with K_{ex} for ferrioxamine B picrate extraction (Table 1) illustrates that the extraction constants for these two cations are comparable. This confirms our experimental approach using Mg^{2+} salts for background electrolyte, since competition for the crown ether is negligible for Mg^{2+} and significant for Na^+.

$MHDFB^+/Mg^{2+}//$Picrate (VIII). The calculations for M = Al(III), Ga(III), and In(III) were performed in the same way as for the $FeHDFB^+$ extraction experiments. Plots of D_{MHDFB^+} versus $\{[pic^-]_{aq}[CE]_{org}\}$ for all four metal complex extractions are shown in Figure 1. The linearity of the plots confirms the equilibrium stoichiometry shown in eq 2. The $K_{ex}^{RNH_3^+,CE,pic^-}$ values obtained from the slopes of these plots according to eq 12 are compiled in Table 1.

Distribution Equilibria. Distribution equilibria (K_d) between the aqueous and chloroform phases were determined at constant ionic strength by carrying out the overall extraction experiment in the absence of DC-18-C-6. The distribution of magnesium picrate into the chloroform phase was negligibly small so that K_d values for RNH_3^+ (where $RNH_3^+ = NH_4^+$ (III), $CH_3(CH_2)_4NH_3^+$ (IV), H_4DFB^+ (V), and $MHDFB^+$ (VI and VIII)) were readily determined from measurements of $[RNH_3^+,pic^-]_{org}/[RNH_3^+]_{aq}$ at a fixed $[pic^-]_{aq}$ as shown in the following equation.

$$RNH_3^+{}_{aq} + pic^-{}_{aq} \rightleftharpoons (RNH_3^+,pic^-)_{org} \qquad K_d \quad (14)$$

$$K_d = [RNH_3^+,pic^-]_{org}/\{[RNH^{3+}]_{aq}[pic^-]_{aq}\} \quad (15)$$

Values for K_d, determined as described in the Experimental Section, are compiled in Table 1.

Host–Guest Equilibria. Values for host–guest association constants, K_a for the reaction

$$(RNH_3^+,pic^-)_{org} + CE_{org} \rightleftharpoons (RNH_3^+,CE,pic^-)_{org} \qquad K_a \quad (16)$$

were calculated from $K_{ex}^{RNH_3^+,CE,pic^-}$ and K_d according to eq 17.

$$K_a = (K_{ex}^{RNH_3^+,CE,pic^-})/K_d \quad (17)$$

The host–guest association constants, including values corresponding to equilibrium 1 for $MHDFB^+$ in $CHCl_3$ solution, are tabulated in Table 1.

Discussion

An important qualitative observation resulting from this study is that DC-18-C-6 can recognize an uncomplexed protonated amine side chain on the surface of a stable metal complex by the formation of a host–guest complex in the second coordination sphere. Furthermore, the formation of a supramolecular assembly results in enhanced extraction of the hydrophilic complex into a lipophilic chloroform phase. Our results also allow us to quantify this host–guest interaction and the extraction from aqueous to organic phase.

The experiments reported here involve measurements of the extraction of various substituted alkylammonium ions (RNH_3^+ and $MHDFB^+$) from an aqueous phase to a chloroform phase by DC-18-C-6. The extraction equilibria shown in eqs 2 and 4 are influenced by the distribution equilibrium (K_d) shown in eq 14 and the host–guest complex stability equilibrium (K_a) shown in eq 16. This is further illustrated algebraically in eq 17. Analysis of the crown ether/chloroform extraction data in this way allows us to identify the factors which influence the extraction equilibrium.

Distribution Equilibria. One may assume that the distribution of a molecule between organic and aqueous phases in the absence of a crown ether (K_d) is essentially determined by its hydrophobicity. The K_d values reported in Table 1 for RNH_3^+ are consistent with values reported in the literature.[48] As R changes from hydrogen to a more lipophilic hydrocarbon chain, the value for K_d increases as expected.

The metal free ligand deferriferrioxamine B may be viewed as a pentylamine ($CH_3(CH_2)_4NH_3^+$; Table 1) derivative substituted with a linear hydrocarbon chain containing three hydroxamate and two amide functional groups. Clearly these hydrophilic substituents, which are probably highly solvated by water, significantly decrease K_d for H_4DFB^+ relative to $CH_3(CH_2)_4NH_3^+$ (Table 1). However, K_d increases by roughly an order of magnitude when the hydroxamate groups of H_4DFB^+ are coordinated to M(III) (M = Al, Fe, Ga, In; Table 1). In the $MHDFB^+$ complex the polar hydroxamate groups are bound to the metal and are not exposed to the solvent medium.

Host–Guest Equilibria. Donor–acceptor complex formation between different crown ethers and ammonium and alkylammonium ions have been reported in the literature at a variety of conditions.[9,10,44,48] Due to the range of experimental conditions and the variety of substituents on the crown ether, a quantitative comparison of the donor–acceptor interactions is often difficult. Nevertheless, in general it may be shown that the donor–acceptor interaction is weakened by the following: (1) replacement of hydrogen in NH_4^+ by other substituents, which results in less hydrogen bonding to the crown ether; (2) substitution of branched chain alkyl groups in RNH_3^+ which cause steric hindrance; and (3) inclusion of electron donating substituent groups on the amine which weaken hydrogen bonding to the crown ether through an electronic effect.[9,10,27,44,50–55]

These points are illustrated by the K_a values obtained in our laboratory for NH_4^+ and RNH_3^+ (Table 1). Replacement of a H by CH_3 decreases K_a. Replacement by an electron releasing longer chain hydrocarbon further reduces K_a, and when substituted by a bulky branched chain hydrocarbon K_a is diminished even more. When a linear chain containing three hydroxamic acid groups is added to the five carbon chain of $CH_3(CH_2)_4NH_3^+$ to produce deferriferrioxamine B (H_4DFB^+) the K_a value is further decreased. Apparently deferriferrioxamine B behaves as a bulky molecule. This may be due to the trihydroxamic acid chain and/or a hydrogen bonded water sheath that is transported into the organic phase. Although deferriferrioxamine B is a linear molecule, in the organic phase it may be organized in a closed, almost cyclic structure where the hydroxamic acid groups are oriented toward each other *via* an intramolecular hydrogen bonding interaction. The assertion that H_4DFB^+ is a bulky molecule is supported by the observation that its K_a value is even lower than that of *t*-$BuNH_3^+$ (Table 1). When the metal complex $MHDFB^+$ is attached to the five carbon chain the K_a value is further diminished. It appears, as discussed below, that steric factors associated with a second coordination shell of water which is carried with the complex into the organic phase may be responsible for this behavior.

(50) Izatt, R. M.; Terry, R. E.; Haymore, B. L.; Hansen, L. D.; Dalley, N. K.; Avondet, A. G.; Christensen, J. J. *J. Am. Chem. Soc.* **1976**, *98*, 7620–7625.
(51) Izatt, R. M.; Lamb, J. D.; Swain, C. S.; Christensen, J. J.; Haymore, B. L. *J. Am. Chem. Soc.* **1980**, *102*, 3032–3034.
(52) Wada, F.; Ishihara, R.; Kamohara, Y.; Matsuda, T. *Bull. Chem. Soc. Jpn.* **1979**, *52*, 2959–2961.
(53) Barret, A. G. M.; Lana, J. C. A. *J. Chem. Soc. Chem. Comm.* **1978**, 471–472.
(54) Behr, J.-P.; Lehn, J.-M.; Vierling, P. *Helv. Chim. Acta* **1982**, *65*, 1853–1867.
(55) Izatt, R. M.; Izatt, N. E.; Rossiter, B. E.; Christensen, J. J.; Haymore, B. L. *Science* **1978**, *199*, 994–996.

Extraction Equilibria. The tetrahedral NH_4^+ cation, with a diameter of 2.86 Å, is well matched for interaction with the cavity of an 18-crown-6 crown ether with a diameter of 2.6–3.3 Å.[6] Thus our work shows a significantly larger chloroform extractability for NH_4^+, relative to Na^+. The $K_{ex}^{RNH_3^+,CE,pic^-}$ value for NH_4^+ listed in Table 1 ($\log K_{ex} = 5.30$) is in excellent agreement with literature data ($\log K_{ex} = 5.43$).[48]

Our results with pentylamine show that replacement of hydrogen in NH_4^+ with a lipophilic alkyl chain enhances the hydrophobic nature of the cation and increases the extraction equilibrium constant by 1.58 log units. Apparently the hydrophobic nature of this cation compensates for (1) the decrease in hydrogen bonding to the crown ether, (2) the electron-donating effect of the CH_2 groups, and (3) steric hindrance. All of these factors contribute to a decrease in host–guest complex stability. On the other hand, when H is replaced by a hydrocarbon chain that has three hydroxamate groups and two amide groups (H_4-DFB$^+$), the $\log K_{ex}$ value drops by 2.4. The extraction equilibrium constant of FeHDFB$^+$ complex has been found to be higher than for ligand alone. The hydrophobic nature of the protonated amine cation is increased, because the hydroxamate groups are now complexed to the metal center. $K_{ex}^{RNH_3^+,CE,pic^-}$ is a product of K_d and K_a (eq 17) and thus cannot distinguish between factors that govern association and distribution.

Metal Complexes, MHDFB$^+$. It is known that Fe(III), Ga(III), and Al(III) form isomorphous tris complexes with mono-[18,19] and trihydroxamic acids.[20] Since In(III) is a d^{10} spherically symmetrical metal ion like Al(III) and Ga(III), and since there are similarities in their coordination chemistry,[14,15,56] it is expected that In(III) will also form a complex with HDFB^{2-} which is a structurally similar analogue of ferrioxamine B. If structurally related steric factors dominated their relative extraction constants, all four complexes should exhibit similar, if not equal, extractabilities in the presence of crown ether, and there would be no reason for the observed differences in distribution constants (K_d) in the absence of crown ether. Therefore, the differences in one log unit of $K_{ex}^{MHDFB^+,CE,pic^-}$ on changing from the Al(III) to the In(III) complex can be attributed to the differences in the metal centers themselves. All four MHDFB$^+$ complexes exhibit a linear relationship between $\log K_{ex}$, $\log K_a$, $\log K_d$, and $1/r_i$, where r_i is the ionic radius of the metal. These linear relationships and the relative magnitudes of the constants suggest the following. First, the driving force for the extraction of the metal complexes from a hydrophilic to a hydrophobic environment is complexation of the protonated amine group by the crown ether. ΔG_{ex} is negative, while ΔG_d is positive (Figure 2), which illustrates the minimal driving force for the distribution of the complexes between the aqueous and chloroform layer in the absence of crown ether. Second, essentially the same factor(s) determine(s) the $K_{ex}^{MHDFB^+,CE,pic^-}$ values for all MHDFB$^+$ complexes and distinguish(es) among the extractabilities of the complexes in the presence and in the absence of crown ether.

The K_d values differ among all metal complexes by a factor of 4, while $K_{ex}^{MHDFB^+,CE,pic^-}$ values differ by a factor of 10. $K_{ex}^{MHDFB^+,CE,pic^-}$ values represent the combined effect of both hydrophilic/hydrophobic interactions (K_d) and steric hindrance (K_a) (eq 17). Since structural differences are expected to be negligible and should result only in a small effect on complexation to the crown ether, differences in K_a suggests the metal complexes are partly hydrated in the organic phase. A different degree of hydration in the second coordination sphere, besides affecting distribution, may impose a different steric effect on the approach of crown ether to the terminal amine group of the bulky metal complexes and therefore influence K_a. Second coordination shell hydration effects are known to be present for metal complexes in organic solvents. For example, it has been established that

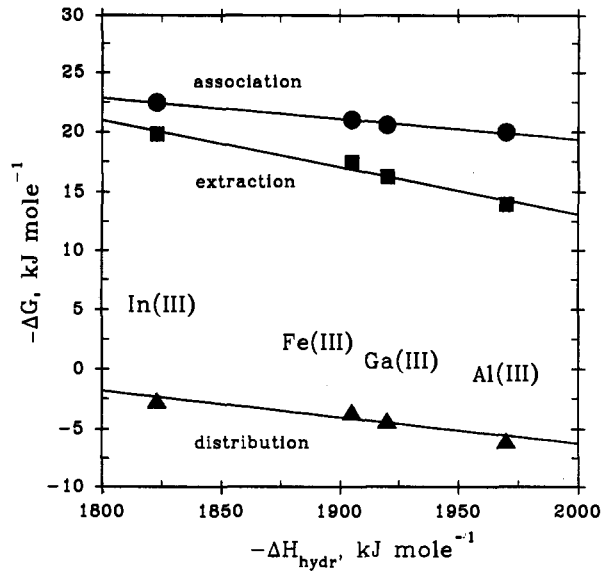

Figure 2. Plots of ΔG as a function of hydration enthalpies (ΔH_{hydr}) for $M(H_2O)_6^{3+}{}_g$ for the distribution (ΔG_d, triangles), extraction (ΔG_{ex}, squares), and host–guest complex formation (ΔG_a, circles) of MHDFB$^+$ (M = In(III), Fe(III), Ga(III), and Al(III)) according to equilibria 14, 5, and 16, respectively.

$Al(H_2O)_6^{3+}$ is so highly hydrated in the second coordination sphere by strong hydrogen bonds that this second coordination shell structure persists even when the total amount of water is small.[57] Recent work by Inoue *et al.*[58] demonstrates that lanthanoid ions, bearing the same 3+ charge as the ions used in our investigation, are incompletely dehydrated when extracted with picrates by 18-C-6 into CH_2Cl_2, in contrast with alkali picrates[41,59] which are almost completely dehydrated upon extraction with crown ether. It is reasonable to assume that a certain degree of hydration of the MHDFB$^+$ complex may persist in the organic phase, although certainly not to the extent found for the hexaaquo ions. Whatever effect contributes to the differences in K_a, it may account for the differences in slopes of the K_{ex} *vs* $1/r_i$, and K_d *vs* $1/r_i$ plots, which differ by a factor of ~2 (slope K_d > slope K_{ex}).

The extraction of MHDFB$^+$ complexes into the organic phase is accompanied by some degree of desolvation. Therefore, the free energy of hydration may correlate with the free energy of the extraction of the complexes. One may expect that all four metal hexaaqua ions bind 10–12 water molecules in their second coordination shell,[60] but the free energy of their solvation is difficult to predict. The only rather closely related process for which free energy can be calculated is the hydration of $M(H_2O)_6^{3+}{}_g$ ions defined by eq 18

$$M(H_2O)_6^{3+}{}_g \rightleftharpoons M(H_2O)_6^{3+}{}_{aq} \qquad \Delta H_{hydr} \qquad (18)$$

We can use the Born equation to calculate the solvation enthalpies for this process (ΔH_{hydr}), taking into account that the entropy change for this process is negligible at room temperature.[61,62] The linearity of the plots of $\log K_{ex}^{MHDFB^+,CE,pic^-}$, K_a, and K_d vs $1/r_i$ and $\Delta G_{ex}^{MHDFB^+,CE,pic^-}$, ΔG_a, and ΔG_d *vs* ΔH_{hydr} (Figure 2) suggests that the hydration enthalpies of the MHDFB$^+$ complexes parallel the hydration enthalpies of the $M(H_2O)_6^{3+}$ ions. This suggests that there are differences in hydration shells caused by

(56) Mulla, F.; Marsicano, F.; Nakani, B. S. *Inorg. Chem.* **1985**, *24*, 3076–3080.
(57) Caminiti, R.; Licheri, G.; Pinna, G. *J. Chem. Phys.* **1979**, *71*, 2473–2476.
(58) Inoue, Y.; Nakagawa, K.; Hakushi, T. *J. Chem. Soc., Dalton Trans.* **1993**, 1333–1336.
(59) Takeda, Y.; Goto, H. *Bull. Chem. Soc. Jpn.* **1979**, *52*, 1920–1922.
(60) Reynolds, W. L.; Reichley-Yinger, L.; Yuan, Y. *Inorg. Chem.* **1985**, *24*, 4273–4278.
(61) Born, M. *Z. Phys. Chem.* **1920**, *1*, 45–48.
(62) Reynolds, W. L.; Vumry, R. W. *Mechanisms of Electron Transfer*; The Ronald Press Company: New York, 1966.

the different M^{3+} ions in $MHDFB^+$ which dictate the differences in K_d and K_a. Therefore, the more tightly held second coordination shell water molecules for the smaller M^{3+} ions in $MHDFB^+$ cause a decrease in K_d. That is, the surface of the complex is more hydrophilic for the smaller M^{3+} ions studied. These second coordination shell water molecules also provide a steric hindrance to host–guest complex formation, thereby decreasing K_a. This analysis supports the assertion that differences in complex hydrophilicities may be the key factor in distinguishing among the transport of different metal complexes across a lipophilic membrane by the means of supramolecular assembly formation with host molecules.

Deferriferrioxamine B. The metal free ligand, H_4DFB^+, which exhibits a low distribution constant K_d, has a $K_{ex}^{H_4DFB^+,CE,pic^-}$ value comparable to the $K_{ex}^{MHDFB^+,CE,pic^-}$ values for the metal complexes $MHDFB^+$. This is because H_4DFB^+ is a sterically more suitable guest molecule for host–guest complexation (K_a), which compensates for the low distribution constant (K_d). This suggests that in biological systems, it may be that deferriferrioxamine B is not transported across a lipid membrane from an aqueous environment unless it is either coordinated to a metal center or is associated with a transport molecule in the source phase or at the cell surface. Furthermore, the low distribution constant (K_d) for deferriferrioxamine B will be a driving force for its release from the cell as soon as the metal is released and incorporated into the metabolic process. These results are in agreement with recent investigations of the cellular transport of deferriferrioxamine B as it relates to its use as a therapeutic agent in the treatment of iron overload.[63-66] Although it has previously been thought that deferriferrioxamine B may enter the cell by the means of passive diffusion, recent experimental evidence points to pinocytosis as the probable mechanism for H_4DFB^+ inclusion in the cell membrane. Such evidence suggests the lack of a specific host–guest system for metal-free H_4DFB^+. This suggests a need to reevaluate previous views of the mechanism by which deferriferrioxamine B (Desferal) removes iron from humans with pathological disorders involving iron overload and iron decompartmentalization.[66] The *n*-octanol/water (TRIS-HCl, pH = 7.4) partition coefficient for deferriferrioxamine B is 0.01 compared to 1.35 for 3-hydroxy-2-methyl-1-*n*-propylpyridin-4-one.[64,66] When no specific association with a transport agent occurs at the cell surface, hydrophobicity, as measured by a partition coefficient, plays an important role in metal chelator transport. Therefore, hydroxypyridone is much more efficient than deferriferrioxamine B in chelating intracellular iron and consequently removing it from the body.[66]

Acknowledgment. We are grateful for the support of the donors of the Petroleum Research Fund, administered by the American Chemical Society, and of NSF (CHE-9113199). We thank Dr. B. A. Moyer (ORNL) for stimulating discussions in the early phase of this work and Dr. M. Biruš (University of Zagreb, Croatia) and E. G. Olmstead, Jr. (Duke University) for their interest and helpful discussions.

(63) Toffa, S.; Cheetman, K.; Fuller, B.; Gower, J.; Green, C. *Biochem. Soc. Trans.* **1991**, *19*, 217S.
(64) Rice-Evans, C.; Baysal, E.; Singh, S.; Jones, S.-A.; Jones, J. G. *FEBS Lett.* **1989**, *256*, 17–20.
(65) Lloyd, J. B.; Cable, H.; Rice-Evans, C. *Biochem. Pharmacol.* **1991**, *41*, 1361–1363.
(66) Porter, J. B.; Gyparaki, M.; Burke, L. C.; Huehns, E. R.; Sarpong, P.; Saez, V.; Hider, R. C. *Blood* **1988**, *72*, 1497–1503.